TABLE I. The EFG/strain tensor for NaCl.

	S_{11} (a.u.)	S_{44} (a.u.)
Calculated	+0.85	−0.43
Experiment[a,b]	0.82 ± 0.12	0.34 ± 0.03

[a]See Ref. 7.

[b]The signs of S_{11} and S_{44} were not determined experimentally, but were assumed to be opposite.

ion wave functions. This is probably the first calculation of an EFG in any solid that has not required the use of any Sternheimer shielding factors. The method can be applied to other solids and complex molecules and to other hyperfine interactions. Further studies are needed to determine the limits of validity of the model and to consider possible refinements in the case of more covalent solids.

The author wishes to thank the staff of the Queen's University Computing Centre for their help, and C. Hodges for his comments on the manuscript.

*Research supported by the National Research Council of Canada.

[1]D. R. Taylor, J. Chem. Phys. 48, 536 (1968).

[2]R. R. Sharma, Phys. Rev. Lett. 25, 1622 (1970). Similar calculations are reported by R. R. Sharma, Phys. Rev. Lett. 26, 563 (1971); R. R. Sharma and B. N. Teng, Phys. Rev. Lett. 27, 679 (1971); and by D. Sengupta, J. O. Artman, and G. A. Sawatzky, Phys. Rev. B 4, 1484 (1971). See also a recent criticism of these calculations by R. M. Housley and R. W. Grant, Phys. Rev. Lett. 29, 203 (1972).

[3]R. M. Sternheimer, Phys. Rev. 84, 244 (1951).

[4]C. A. Coulson, *Valence* (Oxford Univ. Press, Oxford, England, 1961).

[5]R. L. Matcha, J. Chem. Phys. 48, 335 (1968). This article contains references to similar computations on other alkali-halide molecules by Matcha.

[6]A. D. McLean and M. Yoshimine, IBM J. Res. Develop. 12, 206 (1968).

[7]J. L. Marsh, Jr., and P. A. Casabella, Phys. Rev. 150, 546 (1966). These and other experiments measure the product of EFG and the nuclear quadrupole moment. The Na^{23} quadrupole moment has been recently determined to be $(0.101 \pm 0.008) \times 10^{-24}$ cm^2 [R. M. Sternheimer and R. F. Peierls, Phys. Rev. A 3, 837 (1971)].

[8]Confusion may arise in regard to the meaning of the term "molecular wave functions." In this Letter it refers to solutions of the Schrödinger equation for a diatomic molecule. In the literature this term as well as "molecular orbitals" may often refer to wave functions for a molecule or cluster obtained by assigning free-ion wave functions to each electron, the only modification being to require orthogonality between one-electron states.

X-Ray Photoemission Spectra of Crystalline and Amorphous Si and Ge Valence Bands*

L. Ley,† S. Kowalczyk, R. Pollak,‡ and D. A. Shirley
Department of Chemistry and Lawrence Berkeley Laboratory, University of California, Berkeley, California 94720
(Received 13 July 1972)

High-resolution x-ray photoelectron spectra of the total valence bands of crystalline and amorphous silicon and germanium are reported. For the crystals, the spectra yield results that are strikingly similar to current theoretical calculations of the electron density of states, $\rho(E)$. Amorphous Si and Ge exhibit definite band structures that are similar to one another but markedly different from the crystalline results. They agree very well with the theoretical model of Joannopoulos and Cohen.

Although several density-of-states calculations have been carried out on silicon[1] and germanium,[2] relatively little experimental information is as yet available concerning the densities of states $\rho(E)$ of the more tightly bound valence electrons of these semiconductors. The valence-band densities of states of the crystalline modifications of Si and Ge are of current and continuing interest. In addition, a considerable amount of recent activity has been directed toward elucidating the electronic structure in the amorphous forms.[3] Thorpe and Weaire[4] have discussed three alternative models for the densities of states of amorphous Si and Ge, and Joannopoulos and Cohen[5] have recently given quantitative predictions for $\rho(E)$. In this Letter we present the first high-resolution x-ray photoelectron (XPS) spectra for the densities of states of crystalline and amor-

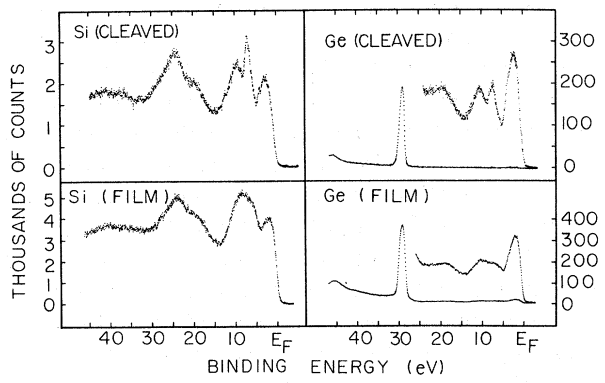

FIG. 1. XPS valence-band spectra of crystalline and amorphous Si and Ge.

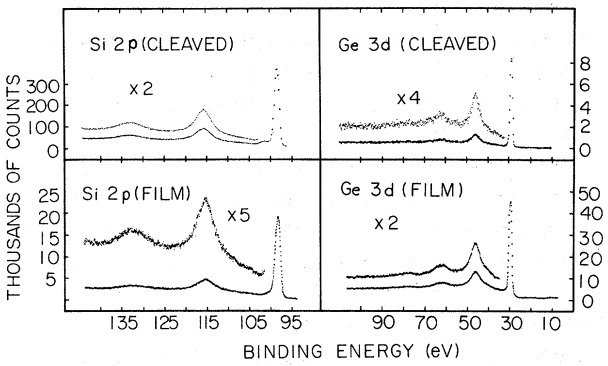

FIG. 2. Si $2p$ and Ge $3d$ core levels exhibiting the characteristic energy-loss structure (plasmons) used in the valence-band correction procedure.

phous Si and Ge and compare these spectra with theory.

The crystalline samples were cleaved in a dry inert atmosphere from 20-Ω cm n-type silicon and intrinsic Ge single crystals. The spectra were taken with a Hewlett Packard HP5950A photoelectron spectrometer with monochromatic Al $K\alpha$ x rays. After cleaving, the samples were introduced into the analyzer vacuum of 8×10^{-9} Torr within 30 sec. The intensity ratios of the Si($2p$) to the contaminant O($1s$) and C($1s$) lines were 5:1 and 12:1, respectively. No oxygen contamination was detected on the Ge sample, whereas the intensity ratio of Ge($3p$) to C($1s$) was 10:1. To prepare amorphous specimens, Si and Ge films were evaporated onto clean gold surfaces at room temperature in the spectrometer sample preparation chamber. The background pressure was initially 4×10^{-7} Torr; it rose to 3×10^{-6} Torr for 4 min during the evaporations. The films were then directly transferred to the analyzer vacuum of 8×10^{-9} Torr. The only contaminant detected was oxygen on the Si film [Si($2p$):O($1s$) = 7:1]. The raw data for the valence-band regions of all four specimens are shown in Fig. 1. The spectra are referenced to the Fermi level E_F of a thin layer of Au evaporated, after the valence-band measurement, onto the semiconductor surfaces. The Au $4f$ lines are used as a secondary standard, by assuming that their binding energies are the same relative to E_F in the evaporated film and in bulk gold. The densities of states of the semiconductors extend ~15 eV below E_F in both Si and Ge. The structure at the foot of the unresolved Ge $3d$ doublet can be entirely assigned to the first characteristic energy-loss structure of the valence-band photoelectrons, as can most of the satellite structure that is found at 17 eV below the valence-band peaks in Si. The energy-loss spectra from typical core levels are shown in Fig. 2. To correct for energy losses, the inelastic loss spectrum was approximated by the sum of a continuous tail with magnitude at each point proportional to the spectrum area at lower bind-

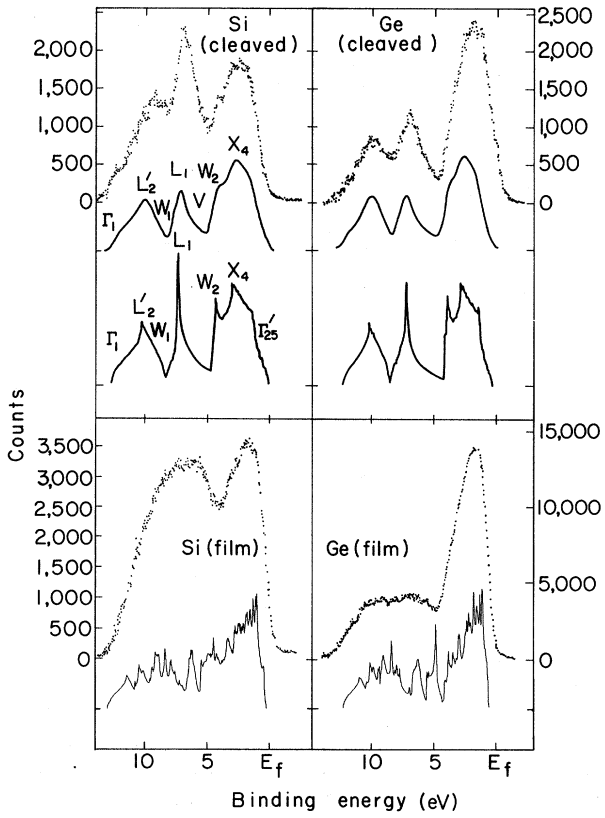

FIG. 3. Point plots, corrected spectra $I'(E)$; lower curves, calculated (Refs. 1c, 2b, and 5) densities of states $\rho(E)$ for the valence bands of crystalline and amorphous (ST-12) Si and Ge; middle curves, broadened $\rho(E)$ spectra for crystalline Si and Ge.

ing energy plus a discrete loss structure constructed by folding a response function determined from the discrete inelastic structure of a sharp core peak and the valence-band structure. This correction accounted for the structure at 19 eV in Ge and for 95% of the structure at 23 eV in Si. The remaining 5% is accounted for by the contaminant oxygen 2s peak. A correspondingly small portion of the peak at 6.6 eV can be attributed to the O(2p) line. The corrected valence-band spectra are shown in Fig. 3.

Several band-structure calculations have predicted $\rho(E)$ for crystalline Si and Ge. These calculations show very good agreement among themselves. They yield three characteristic peaks in $\rho(E)$. We shall label these peaks according to the symmetry points X_4, L_1, and L_2', in order of increasing binding energy. Of course the peaks do not arise entirely from bands at these symmetry points. This notation is used only for identification. To facilitate comparison with experiment we have plotted (Fig. 3) for Si and Ge both $\rho(E)$ as calculated[1c,2b] and a broadened version that is consistent with the experimental resolution.

The agreement between theoretical and experimental peak positions and shapes is striking for crystalline Si and Ge. Table I lists the energies of the characteristic features, the theoretical

TABLE I. Energies of characteristic features in the valence-band spectra of Si and Ge. The theoretical entries are taken from density of states calculations after appropriate broadening.

	Crystalline silicon		
	Experiment[a]	Theory[b]	
	I' (E) (eV)	EPM (Cohen[c]) (eV)	SCOPW (Stukel[d]) (eV)
X_4	2.2	2.6	2.5
W_2	3.6	4.0	3.1
V[e]	4.4	5.1	4.5
L_1	6.6	7.1	6.9
W_1	7.8	8.2	8.2
L_2'	9.2	10.0	9.6
Γ_1	14.7	13.0	11.8

	Crystalline germanium			
	Experiment[a]	Theory[b]		
	I' (E) (eV)	EPM (Cohen[f]) (eV)	OPW (Herman[g]) (eV)	SCOPW (Stukel[d]) (eV)
X_4	2.4	2.3	2.7	2.6
W_2	3.6	3.4	3.8	3.6
V[e]	4.9	4.4	4.9	4.9
L_1	7.2	6.9	7.3	6.8
W_1	8.6	8.5	8.6	7.8
L_2'	10.3	9.7	10.2	9.4
Γ_1	13.0	12.4	12.7	11.7

[a] Positions relative to gold Fermi level.
[b] Positions relative to the top of the valence bands.
[c] See Ref. 1c.
[d] See Ref. 1b.
[e] The valley between W_2 and L_1 is arbitrarily called V.
[f] See Ref. 2b.
[g] See Ref. 2a.

densities of states $\rho(E)$, and the corrected XPS spectra, which we denote as $I'(E)$. The marginal ability to locate the feature W_2 gives an indication of the resolving power of our spectrometer. As Table I shows, $I'(E)$ provides very strong confirmation of all three theoretical methods for calculating $\rho(E)$. The relative intensities of the p-like X_4 and the s-like L_1+L_2' peaks in $I'(E)$ vary markedly between Si and Ge and in neither case agree with $\rho(E)$. This is not unexpected, since $I'(E)$ resembles $\rho(E)$ weighted with the photoemission cross section σ. Extrapolating measured $3s/3p$ and $4s/4p$ core-level intensity ratios[6] to the valence electrons of Si and Ge yields

$$[\sigma(3s)/\sigma(3p)]_{\mathrm{Si}}:[\sigma(4s)/\sigma(4p)]_{\mathrm{Ge}} = 2.3:1.$$

The observed change in the intensity ratio of the corresponding valence-band structures is 2.2:1. Our Si intensities agree well with earlier XPS[7] and Si $L_{2,3}$ [soft x-ray emission spectroscopy (SXS)] results.[8]

The excellent agreement observed for crystalline Si and Ge provides a firm basis for further XPS and theoretical band-structure work on semiconductors. It also suggests that these two approaches may profitably be used together.

The results for amorphous Si and Ge are significantly different from the respective crystalline modifications. From the $I'(E)$ spectra (Fig. 3) we note the following observations: (1) The gross variation of intensity with respect to energy is similar for the amorphous and crystalline materials in both elements. (2) The "X_4" peak remains essentially intact from crystalline to amorphous material. (3) The L_1 and L_2' peaks merge into a single broad peak of intermediate energy. (4) $I'(E)$ shows a distinct minimum between the "X_4" peak and the broader peak in the amorphous materials. (5) The centroid of the "X_4" peak shifts toward E_F in each case, by 0.4 eV in Si and 0.5 eV in Ge. (6) The amorphous Ge spectra were in good agreement for samples prepared by evaporation and by Ar^+ ion bombardment (1000 eV, 10 μA for 1 h).

Observations (1)–(3) are in agreement with the Si $L_{2,3}$ (SXS) results of Wiech and Zöpf.[8] Observation (2) is expected because X_4 arises from localized p-like bonding orbitals,[9] which are relatively insensitive to long-range order. Observation (5) is in qualitative agreement with earlier uv-photoemission work.[3a] Pierce and Spicer[3c] have recently emphasized the sensitivity of uv photoemission spectra to the method of sample preparation, but observation (6) indicates that $I'(E)$ for amorphous Ge was reproducible even though the method of sample preparation was varied.

Observations (3)–(5) are the ones that allow a distinction to be made among different theoretical models for amorphous semiconductors.

Thorpe and Weaire[4] have recently discussed three theoretical models for amorphous Si and Ge. The Brust model[10] yields a $\rho(E)$ spectrum. Thorpe and Weaire indicated that the Penn model[11] might apply to amorphous semiconductors. The $\rho(E)$ curve for the Penn model shows no minimum, but rather a (broadened) logarithmic divergence near E_F and a free-electron $\rho(E)$ below. Our data exclude both of these shapes for $\rho(E)$, thereby ruling out these two models as being applicable to amorphous Si and Ge. Our spectra definitely require a model that predicts large changes in the s-like L_1 and L_2' peaks but not in the p-like X_4 peak on going from the crystalline to the amorphous state. Thorpe and Weaire described a model that distinguished between the effects of local and long-range interactions. They sketched a curve for $\rho(E)$ that is in good agreement with our amorphous Si and Ge spectra, especially observations (2)–(4).

A more quantitative comparison with theory is provided by the recent empirical-pseudopotential calculations of Joannopoulos and Cohen[5] on several forms of Ge. Their $\rho(E)$ results for Ge (ST-12), after smoothing to eliminate sharp features associated with long-range order, show very good agreement with our $I'(E)$ curve. They have also calculated Si (ST-12) with similar results. Their $\rho(E)$ curves are shown in Fig. 3. As they pointed out, Ge (ST-12) shows short-range *disorder*, but the peak near E_F still arises from p-like bonding orbitals. Their model predicts the shift of this peak toward E_F [observation (5)]. The crucial feature of the ST-12 structure, according to Joannopoulos and Cohen, is the presence of five- and seven-membered rings. This feature causes the two lower-energy peaks in $I'(E)$ to merge.

In summary, our $I'(E)$ results strongly support the Joannopoulos-Cohen model for amorphous Si and Ge. It appears that future theoretical developments on the band structure of amorphous Si and Ge should be constrained to reproduce the first five observations listed above.

It is a pleasure to acknowledge the generous contributions of Professor Marvin Cohen and Mr. John Joannopoulos to this research. One of us (L.L.) greatly appreciates a grant from the

Max-Kade Foundation.

*Work performed under the auspices of the U. S. Atomic Energy Commission.

†On leave from University of Bonn, Bonn, Germany.

‡In partial fulfillment of Ph. D.

[1a]See, for example, E. O. Kane, Phys. Rev. 146, 558 (1966).

[1b]D. J. Stukel, T. C. Collins, and R. N. Euwema, in *Electronic Density of States, Proceedings of the Third International Materials Research Symposium, Gaithersburg, Maryland, 1969*, edited by L. H. Bennett, National Bureau of Standards Special Publication No. 323 (U. S. GPO, Washington, D. C., 1971).

[1c]M. L. Cohen and J. D. Joannopoulos, private communication.

[2a]See, for example, F. Herman, R. L. Kortum, C. D. Kuglin, and J. L. Shay, in *Proceedings of the International Conference on II-VI Semiconducting Compounds, Brown University, 1967* (Benjamin, New York, 1967).

[2b]M. L. Cohen and J. D. Joannopoulos, private communication.

[2c]M. Cardona and F. H. Pollak, Phys. Rev. 142, 530 (1966).

[3a]See, for example, T. M. Donovan and W. E. Spicer, Phys. Rev. Lett. 21, 1572 (1968).

[3b]D. T. Pierce and W. E. Spicer, Phys. Rev. B 5, 3017 (1972); T. E. Fischer and N. Erbudak, Phys. Rev. Lett. 27, 1220 (1971).

[3c]D. T. Pierce and W. E. Spicer, Phys. Rev. Lett. 27, 1217 (1971).

[4]M. F. Thorpe and D. Weaire, Phys. Rev. Lett. 27, 1581 (1971).

[5]J. D. Joannopoulos and M. L. Cohen, to be published.

[6]K. Siegbahn, C. Nordling, G. Johansson, J. Hedman, P. F. Heden, K. Hamrin, U. Gelius, T. Bergmark, L. O. Werme, R. Manne, and Y. Baer, *ESCA Applied to Free Molecules* (North-Holland, Amsterdam, 1969).

[7]D. W. Langer, Z. Naturforsch. 24a, 1555 (1969).

[8]G. Wiech and E. Zöpf, in Proceedings of the International Conference on Band-Structure Spectroscopy of Metals and Alloys, Glasgow, Scotland, September 1971 (to be published).

[9]J. P. Walter and M. L. Cohen, Phys. Rev. B 4, 1877 (1971).

[10]D. Brust, Phys. Rev. Lett. 23, 1232 (1969).

[11]D. Penn, Phys. Rev. 128, 2093 (1962).

Measurement of Acoustic-Wave Dispersion in Solids

D. Huet, J. P. Maneval, and A. Zylbersztejn
Groupe de Physique des Solides, Ecole Normale Supérieure, Paris 5°, France
(Received 3 August 1972)

By measuring the time of flight of heat pulses using superconducting tunnel junctions, we have obtained the frequency dependence of the energy velocity of acoustic waves in indium antimonide. This yields, with good accuracy, the dispersion relations for long wavelengths.

Dispersion of acoustic waves in a perfect lattice arises from the discreteness of the crystalline array, and becomes important for wavelengths comparable to the dimension of the unit cell.[1] The frequency versus wave-vector relations (ν versus q) can, in general, be obtained from neutron or x-ray scattering data; however, the frequency dependence of the acoustic velocity has not been observed directly in a solid. We present here the measurement of group-velocity dispersion in indium antimonide by means of heat pulses at liquid-helium temperatures.

Acoustic phonons, having energies of a few Kelvin (10^{11} to 10^{12} Hz), can be generated in a crystal by Joule heating of a metallic film evaporated on the surface. The phonons, thus produced in a wide spectrum, propagate ballistically and reach the crystal boundary—each with its own velocity. If the film is excited with a current impulse, the front edge of the heat pulse will signal the arrival of those phonons that have the largest group velocity, and this usually corresponds to the lowest frequency, while later times will correspond to the arrival of dispersed phonons. The available detectors are quadratic and are mainly of two kinds: (i) superconducting bolometers,[2] sensitive to the energy flux irrespective of the frequency content of the heat pulse, and (ii) superconductor-barrier-superconductor tunnel junctions,[3] which are only sensitive to the phonons able to break the Cooper pairs. Therefore, they have a threshold of detection equal to the superconducting energy gap 2Δ, which usually stands inside the spectrum emitted by the metallic film.